Journal of Chromatography A, 1228 (2012) 57–71

Contents lists available at SciVerse ScienceDirect

Journal of Chromatography A

journal homepage: www.elsevier.com/locate/chroma

Review

Fast liquid chromatography: The domination of core–shell and very fine particles

Szabolcs Fekete[a,*], Erzsébet Oláh[b], Jenő Fekete[a]

[a] Budapest University of Technology and Economics, Department of Inorganic and Analytical Chemistry, Szt. Gellért tér 4., 1111 Budapest, Hungary
[b] Chemical Works of Gedeon Richter Plc., P.O. Box 27, Gyömrői út 19-21, 1103 Budapest 10, Hungary

ARTICLE INFO

Article history:
Available online 22 September 2011

Keywords:
Column efficiency
Sub-2 μm particles
Core–shell particles
Very fine particles
Monolith columns

ABSTRACT

Columns packed with sub-2 μm totally porous and sub-3 μm core–shell particles are very widespread nowadays to conduct fast and efficient separations. In order to carry out really fast separations, short (5 cm long) columns are very popular today. The goal of this paper is to review the recent possibilities in fast or "ultra-fast" HPLC by applying short and narrow bore columns packed with modern core–shell and very fine fully porous particles. Efficiency data obtained with these recently commercialized columns from the past few years are collected, discussed and compared in terms of potential separation time and efficiency. The reasons of the success of these columns are presented. This paper also shows that theoretically expected efficiency is sometimes compromised in practical work especially in the case of narrow bore columns. The extra-column dispersion of a given LC system can also dramatically decrease the performance of small columns. It is not possible to utilize the real efficiency of these small columns in spite of their really high intrinsic separation power.

Contents

1. Introduction

Higher separation efficiency and faster speed have always been of great interest in high performance liquid chromatography (HPLC) and have become increasingly important in recent years mainly driven by the challenges of either more complex samples or increasing the numbers of samples. In order to carry out such fast separations the column length must be decreased and the linear velocity of the mobile phase must be increased. The 3–5 cm long, narrow-bore (2–2.1 mm) columns became very popular especially in the field of pharmaceutical analysis [1–4]. Pharmaceutical industry is particularly interested in using rapid and efficient procedures for qualitative and quantitative analysis in order to cope with a large number of samples and to reduce the time required for delivery of results. Reducing analysis time and guarantying the quality of a separation in HPLC, requires high kinetic efficiency. A general approach to increase the separation power is to enhance the column efficiency.

Recent researches have reported both advantages and disadvantages of columns packed with core–shell and totally porous sub-2 μm particles. The goal of this paper is to review the possibilities in fast HPLC by applying new, very efficient columns packed with core–shell and fully porous sub-2 μm particles. Efficiency data obtained with recently commercialized columns are collected and compared in terms of potential separation time. This paper highlights that small columns (e.g., 5 cm × 2.1 mm) offer not evidently

* Corresponding author. Tel.: +36 30 395 6657.
E-mail addresses: szabolcs.fekete@unige.ch, szfekete@mail.bme.hu (S. Fekete).

0021-9673/$ – see front matter © 2011 Elsevier B.V. All rights reserved.
doi:10.1016/j.chroma.2011.09.050

the fastest separation and moreover the theoretically expected efficiency today is compromised especially in the case of narrow bore columns.

2. Trends in fast and high resolution liquid chromatography

2.1. Sub-2 μm particles

On very fine particles (sub-2 and sub-1 μm), due to the narrow peaks, sensitivity and separation are improved at the cost of pressure. Knox and Saleem were the first to discuss the compromise between speed and efficiency [5]. To overcome the pressure limitations of modern HPLC, the groups of Jorgenson [6,7] and Lee [8] manufactured dedicated instrumentation and columns to allow analysis at very high pressures. A new nomenclature has come with the term ultra high pressure or very high pressure liquid chromatography (UHPLC or VHPLC). The first UHPLC system was released in the year of 2004 (Water Acquity UPLC). Since then several UHPLC systems are commercialized and can work up to 1200–1300 bar (18,000–19,500 psi). A critical aspect is the effect of frictional heating at ultra high pressure, causing temperature gradients within the columns. The radial temperature gradient, due to the heat dissipation at the column wall, can cause significant loss in plate count [9,10]. Gritti et al. concluded that both longitudinal and radial temperature gradients are more significant when the column length is decreased [11]. The radial temperature gradient can effectively lead to ~10% loss of efficiency when operating a 5 cm long column close to 1000 bar [12]. When using very fine particles in narrow bore columns another issue is the quality of column packing. The smaller the particle diameter, the greater the difficulty in preparing a well-packed column bed is [13]. Particle aggregation, frit blockage, particle fracture are all issues when high pressure is required to pack sub-3 μm particles into narrow bore columns [14]. The efficiency of the same particles packed in standard and narrow bore columns could be significantly different. When the same stationary phase is packed in 2.1 mm diameter column, these columns achieve considerably lower plate counts than those having an internal diameter of 3 or 4.6 mm [15,16].

Now columns packed with 1.5, 1.7, 1.8, 1.9 and 2 μm fully porous particles are commercially available and applied with great success in pharmaceutical, biomedical and environmental analysis [17–24]. Several studies proved the excellent efficiency of sub-1 μm particles, however they are not so widespread yet because of the generated very high pressure and the difficulties in column packing [6,7,25–27]. Thoelen et al. reported the use of self-synthesized submicron mesoporous silica materials of 2.4 nm pore diameter in chiral HPLC [28]. Nonporous and porous particles are the two major types of spherical packing materials that have been used for fast HPLC [6,27,29–33]. The major difference between porous and nonporous particles is that porous particles have a resistance to mass transfer contribution from the stagnant mobile phase in the pores. Decreasing the particle size and increasing the diffusion coefficient can improve the mass transfer of solutes in the stagnant mobile phase. Very fine 1.5 μm nonporous silica particles such as Micra C18 have been used in UHPLC systems [34]. Issaeva et al. showed an extremely high speed separation of proteins and peptides using the 1.5 μm Micra particles [35]. Barder et al. presented that the column efficiency of nonporous silica particles (1.5 μm) was considerably higher than that of porous particles (3.5 μm) especially at high flow-rates [30]. Nonporous particles can provide lower mass transfer resistance and higher efficiency than porous particles but porous particles have greater surface areas and can provide much higher sample loading capacity. Seifar et al. estimated a 50-fold sample capacity for porous particles than nonporous particles of the same size [36]. According to Wu et al. the loading capacity for 1.7 μm Acquity C18 porous particles is approximately 16.5 times larger than for Micra C18 nonporous 1.5 μm particles [34]. Another issue is the very low retention on nonporous particles compared to totally porous ones. The average carbon load for 1.5 μm Micra C18 nonporous particles is about 56-times lower than it is for 1.7 μm Acquity C18 porous particles [34]. The lower carbon load means a lower phase ratio for nonporous particles, which leads to significantly lower retention.

2.2. Core–shell particles

In the recent development of particle technology targeted for liquid chromatography, the use of shell particles has received considerable attention. Shell particles manifest the advantages of porous and nonporous particles. First, Knox recommended the use of thin films of the stationary liquid phase in liquid–liquid chromatography [37]. The concept of superficial or shell stationary phases, was introduced by Horváth and co-workers in the late 1960s [38,39]. Horváth applied 50 μm glass bead particles covered with styrene-divinylbenzene based ion exchange resin and became known as pellicular packing material. Later Kirkland presented, that 30–40 μm diameter superficially porous packing provide much faster separations, compared with the large porous particles used earlier in liquid chromatography [40]. Later on the core diameter was reduced and the thickness of active layer was cut to 0.5 μm and was used for fast separation of peptides and proteins [41]. Now fused-core packing materials are commercially available in different diameters (5 μm, 2.7 μm, 2.6 μm and 1.7 μm). The 5 μm Poroshell™ particles consist of a 4.5 μm nonporous core and a 0.25 μm porous silica layer, and the 2.7 μm Halo™ or Ascentis Express™ and Poroshell-120 particles consist of a 1.7 μm nonporous core and a 0.5 μm porous silica layer. Sub-3 μm and sub-2 μm shell particles with very thin porous layer were released in the year of 2009 (2.6 μm and 1.7 μm Kinetex™ particles). This Core–Shell™ technology provides particles, which consist of a 1.9 μm or 1.24 μm nonporous core and a 0.35 μm or 0.23 μm porous silica layer, respectively. Other vendors launched similar sub-3 μm shell packings in the year of 2011 (Accucore, Nucleoshell, SunShell). Table 1 summarizes the particle structure and stationary phase chemistry of the latest generation shell packings. Studies have proven [42] that in the case of 2.7 μm fused-core packing (Halo, Ascentis Express), the peak broadening is larger than expected. It can be explained by the rough surface of particles in which the mass transfer rate is reduced through the outer stagnant liquid film [43]. The new Halo-ES-peptide (16 nm average pore size) column, designed to resolve mixtures of large molecules, provide markedly better kinetic performance than did the first generation of Halo particles (Halo 9 nm) [44]. While this benefit is hardly visible with small molecules, the improvement is more significant with peptide and protein molecules. The kinetic performance for insulin of the 2.7 μm Halo 16 nm particles appears to be equivalent to that of the recently commercialized 2.6 μm Kinetex 10 nm particles [44]. The latest core–shell particle is branded Eiroshell™ (Glantreo Ltd., Ireland). There are three different structures of Eiroshell 1.7 μm core shell particles as (a) 1.0 μm solid core, 0.35 μm shell thickness, (b) 1.2 μm solid core, 0.25 μm shell thickness, and (c) 1.4 μm solid core, 0.15 μm shell thickness [45]. The thickness of the porous layer plays a major role in governing the porosity of the particles [45].

The actual advantages of columns packed with these new core–shell particles lie in the diminution of both the longitudinal diffusion B coefficient (−20 to −30%) and the eddy dispersion A term (−40%) [46]. The decrease of the B coefficient was expected because a significant fraction of the column volume (20%) is now occupied by non-porous silica through which analytes cannot axially diffuse.

Table 1
Particle structure and stationary phase chemistry of the new generation shell packings.

Vendor	Column/product name	Average particle diameter (μm)	Shell thickness (μm)	Stationary phase chemistry
Advanced Material Technology	Halo	2.7	0.50	C18, C8, HILIC, RP-amide, phenylhexyl, pentafluorophenyl
Advanced Material Technology	Halo Peptide-ES 160 Å	2.7	0.50	C18
Agilent	Poroshell 300	5	0.25	C18, C8, C3
Agilent	Poroshell 120	2.7	0.50	EC-C18, SB-C18
Sigma–Aldrich	Ascentis Express	2.7	0.50	C18, C8, HILIC, RP-amide, phenylhexyl, pentafluorophenyl
Sigma–Aldrich	Ascentis Express Peptide-ES 160 Å	2.7	0.50	C18
Phenomenex	Kinetex	2.6	0.35	C18, XB-C18, C8, HILIC, pentafluorophenyl
		1.7	0.23	
Macherey-Nagel	Nucleoshell	2.7	0.5	RP-18, HILIC
Thermo Scientific	Accucore	2.6	0.50	C18, aQ, RP-MS, HILIC, phenylhexyl, pentafluorophenyl
Sunniest	SunShell	2.6	0.5	C18
Commercially not available	Eiroshell	1.7	0.35	C18
		1.7	0.25	
		1.7	0.15	

In contrast, the diminution of the eddy dispersion term was unexpected. It remains uncertain whether the significant decrease of the *A* term is caused by the tighter size distribution of core–shell (5–7%) versus fully porous (15–20%) particles (decrease of the short-range interchannel velocity biases) or by the decrease of the trans-column velocity biases caused by the visible roughness of the external surface area of the core–shell particles [46,47]. The *C* term of shell particles is also more favourable than that of the fully porous particles especially for large molecules (proteins) however the benefits of core–shell particles mostly lie in the *A* and *B* term.

2.3. High temperature liquid chromatography

Temperature in HPLC also offers a chance to cut the analysis time. Elevating the temperature reduces the viscosity of mobile phase and increases the mass transfer and therefore allows the use of high flow rates. Analysis time can be shortened without the loss of resolution through column heating [48–51]. The term high temperature liquid chromatography (HTLC) was introduced in 1969 [52]. Antia and Horváth showed that increasing the separation temperature is a very efficient tool for large molecule separation [53]. Later on, in 1995, Chen and Horváth presented an extremely fast separation of four proteins at 120 °C in less than 10 s [54]. It is important to mention that preheating of the mobile phase is mandatory when operating columns over 60 °C [55]. The peak shape in HTLC depends significantly on the pre-heater coil size, the injected volume and potentially on the composition of the injected solution [56]. Teutenberg et al. presented data about the temperature difference between the eluent temperature and the temperature of the heating block [57]. The mobile phase cooling after the column is required when using an UV detector in order to avoid baseline noise [58]. HTLC suffers from limitations such as the small number of stable packing materials at temperatures higher than 80 °C as well as the potential degradation of thermolabile analytes and the need to have a constant temperature along the chromatographic system. Therefore, until now, the pharmaceutical industry has not considered this approach in everyday routine. The development of a new generation of silica-based column [59,60] as well as non-silica based ones such as zirconia [61,62], has resulted in increased thermal stability. Polymeric stationary phases can be used up to temperatures of 150 °C, and graphitic carbon columns remain stable up to 200 °C [63]. The achievable reduced plate height (h) of polymeric columns decreased significantly by heating up the column [64]. Efficiencies of more than 130,000 theoretical plates were achieved by connecting up to six columns (in Hidrophilic Interaction Liquid Chromatography, HILIC) of 25 cm each and operating them at elevated temperature [65]. High temperature size-exclusion chromatography (SEC) can be employed as an efficient second-LC in the 2D-LC separation of synthetic polymers [66]. "Isobaric" high temperature chromatography, where the temperature and flow rate follow a gradient program, was developed and evaluated against a conventional organic solvent gradient [67]. A combination of high temperature-ultra high pressure liquid chromatography (HT-UHPLC) is also a promising technique [67]. Some applications of fast HTLC in pharmaceutical analysis is also reported [68].

2.4. Monolithic columns

Monolithic columns were introduced for their potential use at high mobile phase velocities due to decreased mass transfer effects over conventional fully porous particles [69,70]. Since the first experiment of Hjertén with continuous polymer beds [71] monolithic columns get comprehensive attention. The micrometer ranged through pores assure high flow rate with lower pressure drop than packed beds [72,73], while nanometer ranged mesopores provided adequate efficiency for the monolithic columns. Mriziq et al. proved that the local efficiency near the wall of a 10 mm i.d. and 100 mm long silica based monolithic column is lower than the efficiency near the center of the column [74]. This macroscopic heterogeneity can be the reason for the very different minimum plate heights published in the literature [75–77]. The separation efficiency depends on the morphology of the monolithic columns. Skudas et al. found that column efficiency increased with decreasing skeleton diameter but this diminution is limited because of the heterogeneity of the monolithic columns [78]. The group of Minakuchi prepared monolithic octadecylsilylated silica columns with domain size between 2.3 and 5.9 μm and achieved lower reduced plate height with the smaller domain size [75]. Gritti and Guiochon found that the contribution of the *A*-term to the band broadening decreased with increasing mesopore size and molecular diffusivity of the compound because of the fast mass transfer across the column. The *C*-term efficiency is regulated by the mass transfer resistance between the flowing mobile phase and the stagnant eluent in the porous skeleton [76].

Eeltik et al. highlighted that maximum number of plates obtained with monolithic silica columns is higher than obtained with 5 μm particles packed Hypersil column and appropriate number of theoretical plates can be achieved in shorter time with monolithic column applying the same mobile phase [79]. Miyabe

compared fully porous, partially porous such as shell, non-porous spherical particles and full-porous cylindrical fibers such as silica monoliths. The correlation of separation speed with peak capacity was studied and proved that monolithic columns and shell particles are better for fast HPLC than fully and non-porous particles [80].

There are detailed review articles about monolithic columns in HPLC [81], monolithic stationary phases in the microscale separation [82] and in chiral separation [83], therefore here we would like to review only the latest developments. Nowadays monolithic columns are applied in hydrophilic interaction chromatography (HILIC) [84]. Separation factor on zirconia coated silica monoliths showed strong dependence on the ratio of Si–OH and Zr–OH group [85]. Particle-monolithic columns combine selectivity properties of monolithic columns and packed beds and separation efficiency of these columns is between the efficiency of the two combined stationary phases [86]. Lv et al. covalently bonded β-cyclodextrin to an organic polymer monolith and successfully applied for separation of racemic ibuprofen [87]. Causon et al. applied polymer monolithic column at elevated temperature. The decrease in mobile phase viscosity and the low separation impedance of monolithic column allowed to couple three monolithic columns to increase the peak capacity and they separated proteins in a few minutes [88].

3. Comparison of the efficiency and achievable separation speed of different columns, the kinetic plot method

Kinetic plots are neat tools for visualizing the compromise between separation speed and efficiency. Van Deemter, Knox and other h–ν (where h is reduced plate height and ν is reduced linear velocity) plots lack permeability considerations. It is very straightforward to map the kinetic performance potential of a given chromatographic support type by taking a representative set of H–u (where H is plate height and u is linear velocity) data and re-plotting them as H^2/K_{v0} versus $K_{v0}/(uH)$ instead of as H versus u (K_{v0} is the unretained component based column permeability). Multiplying both quantities with the same proportionality constant (being the ratio of the available pressure drop, ΔP, and the mobile phase viscosity, η), the obtained values correspond directly to the minimal t_0-time needed in a column taken exactly long enough to yield a given number of N theoretical plates at the available pressure drop.

N and t_0 can be calculated according to the following equations introduced by Desmet et al. [89]:

$$N = \frac{\Delta P}{\eta}\left(\frac{K_{V0}}{uH}\right) \quad (1)$$

$$t_0 = \frac{\Delta P}{\eta}\left(\frac{K_{V0}}{u^2}\right) \quad (2)$$

where ΔP is the available pressure drop. Column permeability can be determined experimentally using the following relation:

$$K_{V0} = \frac{u\eta L}{\Delta P} \quad (3)$$

where ΔP is the pressure drop over the column with length L. Viscosity values can be calculated using equations derived by Chen and Horvath [90].

Calculation and data transferring to obtain the kinetic plots – presented in this paper – was achieved by using the Kinetic Method Plot Analyser template (Gert Desmet, Vrije University Brussel, Belgium). The non-linear curve fitting to plots was performed using MS Excel (Solver).

4. Possibilities of recent core–shell technology

The initial intend of applying pellicular particles was the analysis of macromolecules. The rational behind this concept was to improve column efficiency by shortening the pathways that analyte molecules must travel and, doing so, to improve their mass transfer kinetics [46]. Recently, the pressing needs to improve analytical throughputs forced the particle manufacturers to find a better compromise between the demands for higher column efficiency and the need for columns that can be operated with the conventional instruments for liquid chromatography (with moderate column back-pressures) [46].

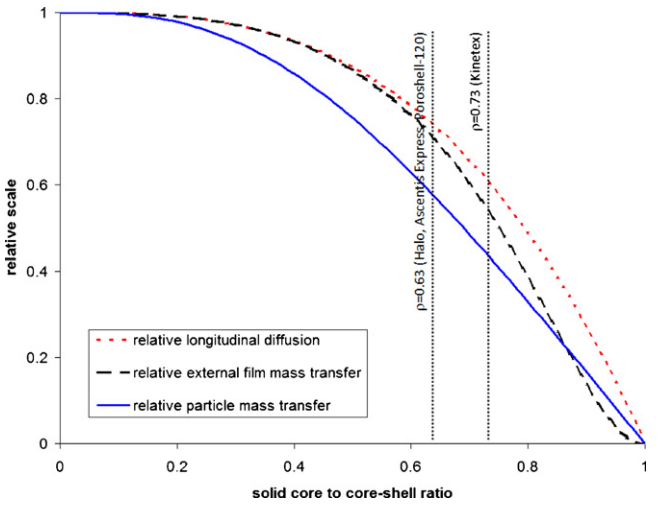

Fig. 1. Change in reduced longitudinal diffusion term (red, dotted curve), in external film mass transfer term (black, dashed curve), and in transparticle mass transfer resistance (blue curve) against the solid core to whole particle ratio in the case of shell particles. (For interpretation of the references to color in this figure legend, the reader is referred to the web version of the article.)

Core–shell particles are made of a solid, nonporous core surrounded by a shell of a porous material that has properties similar to those of the fully porous materials conventionally used in HPLC. Shell particles have a thick porous layer, pellicular ones have a thin layer, although all intermediates are theoretically possible. It is expected that the axial and eddy dispersion contributions to the efficiency of columns packed with these particles would correspond to the external diameter of the particle, but the internal mass-transfer resistances would correspond to the thickness of the porous layer.

Different plate height models are written as the sum of four different contributions such as (1) reduced longitudinal diffusion, (2) eddy dispersion, (3) the external film mass transfer and (4) the transparticle mass transfer resistance. The transparticle mass transfer resistance for shell particles was derived by Kaczmarski and Guiochon [91]. According to this theory the intraparticle diffusivity depends on the ratio (ρ) of the diameter of the solid core to that of the particle in a core–shell particle. As this ratio increases the mass transfer kinetics become faster through the shell particles than it is through totally porous particles.

The reduced longitudinal diffusion term (h_{long}) can be written by the following equation:

$$h_{\text{long.}} = 2\frac{\gamma_e + (1-\varepsilon_e)(1-\rho^3/\varepsilon_e)\Omega}{\nu} \quad (4)$$

where γ_e is the obstruction factor for diffusion in the interparticle volume, ε_e is the interstitial porosity, Ω is the ratio of the intraparticle diffusivity of the sample through the porous shell (D_{shell}) to the bulk diffusion coefficient, and $\rho = Ri/Re$ is the ratio of the diameter of the solid core (Ri) to that of the particle (Re). Fig. 1(red, dotted curve) shows the change of $h_{\text{long.}}$ against the ratio of the diameter of the solid core to that of the whole core–shell particle.

The eddy dispersion term (h_{eddy}) includes sources of four different origins, differing in the length scale considered, e.g., the transchannel ($i = 1$), the short-range interchannel ($i = 2$), the

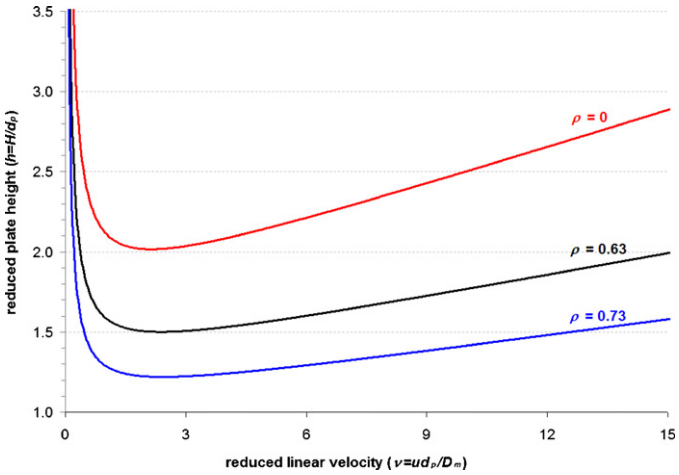

Fig. 2. Theoretical h–ν curves of fully porous and core–shell packing ($\rho = 0$, $\rho = 0.63$ and $\rho = 0.73$). Hypothetical mobile phase composition: 50% acetonitrile–50% water, and analyte molecular weight: 1000 g/mol. No extra-column band broadening is assumed.

long-range interchannel ($i = 3$), and the trans-column flow heterogeneities ($i = 4$). For the eddy dispersion a general expression is given by [92,93]:

$$h_{\text{eddy}} = \sum_{i=1}^{i=4} \frac{1}{(1/2\lambda_i) + (1/\omega_i \nu)} \cong 2\sum_{i=1}^{i=4} \lambda_i \tag{5}$$

The values of $\lambda_1 - \lambda_3$ were estimated by Giddings [92]. The value of λ_4 can be derived from the flow distribution across the column diameter.

The external film mass transfer term (h_{film}) was derived from the Laplace transform of the general rate model equations [94]. It can be expressed as:

$$h_{\text{film}} = \frac{\varepsilon_e}{1-\varepsilon_e} \frac{k_1^2}{(1+k_1)^2} \frac{1}{3Sh} \nu \tag{6}$$

where $Sh = (k_f\, d_p/D_m)$ is the Sherwood number, k_f is the film mass transfer coefficient, and k_1 is given for superficially porous particles by the next formula [89].

$$k_1 = \frac{1-\varepsilon_e}{\varepsilon_e} \left(\varepsilon_p + \frac{1-\varepsilon_p(1-\rho^3)}{1-\rho^3} K_a \right) (1-\rho^3) \tag{7}$$

where ε_p is the porosity of the porous shell of the particle and K_a is the Henry's constant of adsorption on the walls of the porous shells. Fig. 1(black, dashed curve) shows the change of h_{film} against the ratio of the diameter of the solid core to that of the whole core–shell particle.

The transparticle mass transfer resistance (h_{particle}) is given by the following equation [91]:

$$h_{\text{particle}} = \frac{\varepsilon_e}{1-\varepsilon_e} \frac{k_1^2}{(1+k_1)^2} \frac{1}{30\Omega} \frac{1+2\rho+3\rho^2-\rho^3-5\rho^4}{(1+\rho+\rho^2)^2} \nu \tag{8}$$

This equation is consistent with the one applied for totally porous particles when $\rho = 0$. As ρ increases, the apparent intraparticle diffusivity of the probe studied increases and the mass transfer kinetics becomes faster through the shell particles than it is through totally porous particles. Fig. 1(blue curve) shows the change of h_{particle} against the ratio of the diameter of the solid core to that of the whole core–shell particle.

According to this theory, approximately 2.3 and 1.7 times faster intraparticle diffusivity can be expected for commercially available sub-3 μm shell packing (Kinetex and Halo/Ascentis Express/Poroshell-120, $\rho = 0.73$ and $\rho = 0.63$), than for fully porous particles (if the particle size is similar).

Fig. 2 illustrates a comparison of theoretical h–ν curves. The only difference is the solid core to core–shell ratio, all other column properties are assumed to be the same (same particle size, same quality of packing, etc.) when constructing these plots. It can be seen that both plate height and the slope of C term are more favourable for a core shell material than for a fully porous packing. For a well packed column a minimum reduced plate height value of $h_{\text{min}} = 2$ can be expected while core shell columns can perform much lower plate heights. A reduced plate height minimum of $h_{\text{min}} = 1.4$–1.5 can be predicted for shell particles with $\rho = 0.63$, while particles with $\rho = 0.73$ should perform $h_{\text{min}} = 1.1$–1.2 plate height minimum.

A recent study has shown that the ratio of solid core to core–shell, strongly influences the mass transfer kinetic of the column [45]. Glennon and Omamogho presented experimental results on the kinetic efficiency of core–shell particles ($d_p = 1.7$ μm). The Eiroshell™ particles were studied with different solid core to core–shell ratio: (a) 1.0 μm solid core, 0.35 μm shell thickness, (b) 1.2 μm solid core, 0.25 μm shell thickness, and (c) 1.4 μm solid core, 0.15 μm shell thickness. There was an obvious correlation between the h_{min} and shell thickness (see in Table 2). Particles with 0.35 μm shell thickness gave the highest h_{min} value while the particles with the thinnest porous layer (0.15 μm shell) performed the smallest minimum reduced plate height value [45].

Recently Desmet and Deridder transformed Effective Medium Theory (EMT), which applied for thermal and electrical conductivity, to determine longitudinal diffusion in chromatography [95]. EMT equations can be applied for fully porous, porous shell, spherical and cylindrical particles. The theory considers the column as a binary medium, which consists of an interstitial void with a volumetric fraction ε_e and particles with volumetrical fraction of $1 - \varepsilon_e$. It was implied that the solid core reduced the B-term not more than 34% in comparison with fully porous particle [96,97].

In contrast to the theory, several different reduced plate height minimum values were reported in the last 3–4 years obtained with core–shell packing. Table 2 summarizes the minimum reduced plate height values, minimum plate heights and the maximum achievable plate counts of the columns reported in recent papers. All of the reported plate height values were corrected for extra-column peak broadening. It can be seen that 5 cm long columns packed with core–shell particles can achieve a maximum plate count of $N = 9000$–$19{,}000$ when small molecular weight compounds are separated. The ever reported maximum plate number of a 5-cm long core–shell column (Kinetex 1.7 μm) is $N \sim 19{,}200$ [16]. The 10-cm long columns provide plate numbers in the range of $N = 14{,}000$–$32{,}000$ while the 15 cm long columns can achieve $N = 30{,}000$–$44{,}000$. The h_{min} values listed in Table 2 show that the expected maximum efficiency fails in practice, especially in the case of narrow bore columns. The standard bore (4.6 mm ID) Poroshell-120 columns give about $h_{\text{min}} = 1.4$–1.6, it is in good agreement with the theory, but the narrow bore Poroshell-120 columns perform $h_{\text{min}} \geq 2.0$. The 4.6 mm Halo columns provide $h_{\text{min}} = 1.5$–1.7 for small molecules, and 2.1 mm columns packed with this particles perform very similar reduced plate height values ($h_{\text{min}} = 1.6$–1.8). The 2.6 μm Kinetex particles achieve $h_{\text{min}} = 1.2$–1.4 when packed in standard bore column, and $h_{\text{min}} = 1.9$ when packed in narrow bore column (Fig. 3).

The brands of core–shell packing materials made of fine particles are available in both conventional (4.6 mm ID) and narrow-bore (2.1 mm ID) columns. It is a general observation that the efficiency of the former tends to be markedly higher than that of the latter. It was shown that the landmark performance of columns packed with the Kinetex 2.6 μm particles is only limited to the standard bore column (i.e., 4.6 mm), however, when packed in a narrow

Table 2
Summary of reported minimum reduced plate height values, minimum plate height values and maximum plate numbers obtained with different modern core–shell packing.

Stationary phase	Column dimension	h_{min}	H_{min} (μm)	N_{max}	Solute	Reference
2.7 μm Poroshell 120	2.1 mm × 100 mm	2.5	6.8	14,706	Naphthalene	[100]
	2.1 mm × 50 mm	2.0	5.4	9259	Naphthalene	[100]
	4.6 mm × 150 mm	1.4	3.8	39,474	Naphthalene	[100]
	4.6 mm × 100 mm	1.6	4.3	23,256	669 Da compound	[47]
2.7 μm Halo	2.1 mm × 150 mm	1.8	4.9	30,612	Naphthalene	[100]
	4.6 mm × 150 mm	1.6	4.3	34,883	Naphthalene	[100]
	4.6 mm × 150 mm	1.7	4.6	32,609	Anthracene	[103]
	4.6 mm × 150 mm	2.0	5.4	27,778	Bradykinin, lys-bradykinin	[103]
	4.6 mm × 150 mm	~2.0	~5.4	~28,000	Insulin	[103]
	4.6 mm × 150 mm	~2.0	~5.4	~28,000	Lysozyme	[103]
	4.6 mm × 150 mm	~4.0	~10.8	~13,900	BSA	[103]
	4.6 mm × 150 mm	1.8	4.9	30,612	β-Lipotropin	[101]
	4.6 mm × 50 mm	1.7	4.6	10,870	Virginiamycin	[101]
	4.6 mm × 50 mm	2.0	5.4	9259	Insulin	[101]
	2.1 mm × 50 mm	3.4	9.2	5435	Polypeptide 4.1 kDa	[16]
	2.1 mm × 50 mm	1.6	4.3	11,628	Levonorgestrel	[42]
	4.6 mm × 100 mm	1.5	4.1	24,390	669 Da compound	[47]
	2.1 mm × 100 mm	1.8	4.9	20,408	Butyrophenone	[139]
2.6 μm Kinetex	2.1 mm × 150 mm	1.5	3.9	38,462	Naphthalene	[100]
	4.6 mm × 150 mm	1.3	3.4	44,118	Naphthalene	[100]
	2.1 mm × 50 mm	1.9	4.9	10,204	Estradiol	[15]
	2.1 mm × 100 mm	1.9	4.9	20,408	Estradiol	[15]
	3.0 mm × 100 mm	1.3	3.4	29,412	Estradiol	[15]
	4.6 mm × 100 mm	1.2	3.1	32,258	Estradiol	[15]
	4.6 mm × 100 mm	1.2	3.1	32,258	Naphthopyrene	[140]
	2.1 mm × 100 mm	1.5	3.9	25,641	Naphthopyrene	[140]
	4.6 mm × 100 mm	1.4	3.6	27,778	669 Da compound	[47]
1.7 μm Kinetex	2.1 mm × 150 mm	2.9	4.9	30,612	Naphthalene	[100]
	4.6 mm × 100 mm	2.1	3.6	27,778	Naphthalene	[100]
	2.1 mm × 50 mm	3.7	6.3	7937	Polypeptide 4.1 kDa	[16]
	2.1 mm × 50 mm	1.5	2.6	19,231	Estradiol	[16]
	2.1 mm × 50 mm	2.5	4.3	11,628	Naphthopyrene	[141]
Eiroshell 150-C18	2.1 mm × 50 mm	1.9	3.2	15,625	Naphthopyrene	[141]
Eiroshell 250-C18	2.1 mm × 50 mm	2.2	3.7	13,514	Naphthopyrene	[141]
Eiroshell 350-C18	2.1 mm × 50 mm	2.5	4.3	11,628	Naphthopyrene	[141]
2.7 μm HALO-ES	4.6 mm × 150 mm	1.4	3.8	39,474	β-Lipotropin	[101]
	4.6 mm × 150 mm	~2	~5.4	~28,000	Insulin	[101]

bore column (2.1 mm ID), the reduced plate height minimum of 1.9 was achieved [15]. This suggests that the packing of narrow bore columns does not provide comparable packed bed homogeneity to that of the standard bore columns. Gritti and Guiochon studied the mass transfer kinetics of the Kinetex 1.7 μm C18 packed in a 2.1 mm ID column, and the minimum reduced plate height was above 2.0 [98]. This provide further suggestions that the problematic situation of packing narrow bore columns is compounded when the packing materials are very fine such as the sub-2 μm particles. According to Gritti and Guiochon, the difference in efficiency is accounted for a contribution to the column HETP of the long-range eddy diffusion term that is larger in the 2.1 than in the 4.6 mm I.D. columns [99]. While the associated relative velocity biases are of comparable magnitude in both types of columns, the characteristic radial diffusion lengths are of the order of 100 and 40 μm in the wall regions of narrow-bore and conventional columns, respectively [99].

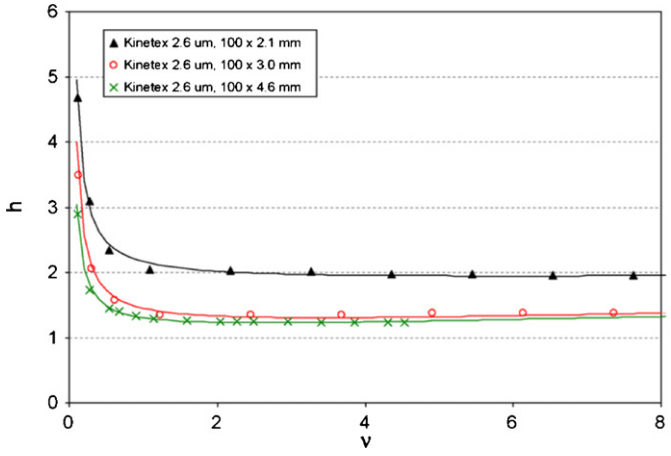

Fig. 3. Experimental h–ν curves of 2.6 μm shell-type (Kinetex, 100 mm × 2.1 mm, 100 mm × 3.0 mm and 100 mm × 4.6 mm), column (peak widths were corrected for the extra-column broadening). Mobile phase: 48% acetonitrile–52% water, temperature: 35 °C, injection: 0.5 μL, $D_M = 1.15 \times 10^{-5}$ cm^2/s. Test analyte: estradiol. From Ref. [15] with permission. The detailed calculations can be found in Ref. [15].

Another observation is, that the 4.6 mm ID beds packed with 2.6–2.7 μm superficially particles are more homogeneous than those of the 2.1 mm ID narrow-bore beds packed with 1.7 μm fully porous particles [99]. The external roughness of the core–shell particles might explain the origin of this advantageous property because the shear stress that takes place during the slurry packing process is stronger between rugged particles than between smooth ones. Therefore, particles move less by respect to each other and the amount of strain occurring through the bed is smaller. Thus, the distribution of the external porosity throughout the bed of rugged particles is more homogeneous from the center (low packing stress) to the wall of the column (high packing stress) than through beds of smooth particles [100].

Some recent studies, focusing on particles with a different design such as the superficially porous particles, have suggested that particles displaying a very narrow particle size distribution

(PSD) can lead to unprecedented low minimal plate heights [101,102]. It is however unclear whether this finding can be purely related, because there are also other factors that might influence the quality of packing. Superficially porous particles have a higher density and some of them are rougher than fully porous particles [101,103]. This might also have had an influence on the achieved packing quality, apart from the PSD.

A strong (nearly linear) correlation has been observed between the width of the particle size distribution of several commercially available HPLC particle types (both fully porous and superficially porous) and some commonly used parameters that reflect the quality of a packing, namely the minimum reduced plate height, the *A*-term and the minimum reduced separation impedance [47]. These observations have been made despite the fact that the studied particles have a number of other differences besides PSD, such as particle porosity, pore size, pore structure and bonding conditions. Covering a wide group of fully porous as well as porous-shell particles, these observations confirm the most recent views in the field, stating that there is a strong relation between the particle size distribution of the packings and the quality of the packing. The observed nearly linear relationship between the PSD and obtained reduced plate height minimum also suggests that the performance of the current generation of fully porous particle columns could be significantly improved if the PSD of these particles could be reduced.

However the original purpose of developing core–shell particles was to separate high molecular weight compounds such as proteins or polymers, these particles show significant advantages also for small molecule separations. Interestingly, it was recently shown that the enhanced performance of columns packed with shell particles in the separation of small molecules was due to the combination of lower longitudinal diffusion (*B* coefficient) and eddy diffusion (*A* coefficient) terms of the general van Deemter equation [102]. Most noteworthy, that small molecular weight compounds diffuse most rapidly, so trans-particle mass transfer resistance in fully porous particles is nearly negligible and does not contribute significantly to the overall plate height around the minimum of the HETP curve [104]. The mass transfer resistance at the solid–liquid interface is mostly accounted for the external film mass transfer resistance [105,106] and, possibly, for the heat friction under very high pressures [98,107]. In conclusion, the recent core–shell packing manifests advantages in both small and macromolecule separations.

The measured reduced plate height minimum values of peptides and proteins were reported in the range of h_{min} = 1.8–4.0. Gritti and Guiochon highlighted the advantage of Halo C18 column in comparison with conventional fully porous 3 μm particles in separation of macromolecules, however the kinetic performance for charged compounds is strongly dependent on both the pH additive and the chemistry of silica surface. The authors used 0.1% trifluoraceticacid (pH ∼ 2) as mobile phase additive in that study for peptide separation. The Halo C18 column provided lower *A*- and *B*-term, but approximately the same *C*-term for low molecules as fully porous bed. The real advantage of core–shell particles is pronounced in separation of compounds with low diffusivities such as proteins or large peptides when the mass transfer kinetics is faster and the *C*-term of the Halo column was about twice lower than that of a column packed with totally porous silica particles [103].

The recently commercialized 5 cm long, narrow bore 1.7 μm Kinetex C18 column provided approximately 50% improvement in plate heights for separation of peptides in comparison with fully porous particles [16]. Reducing the particle size from 2.6 μm to 1.7 μm manifests in 20% improvement in plate heights and optimum linear velocity shifts towards higher values [16].

5. Possibilities of small columns packed with very fine fully porous particles

Halasz et al. demonstrated theoretically that the fastest HPLC separations could be obtained by employing the smallest particles [108]. It was also known that the minimum analysis time that could be achieved for a given separation was limited by the pressure limit of an HPLC system. For a given separation, the separation time is proportional to the theoretical plate height at constant linear velocity for a given retention factor. The use of smaller particles to shorten the analytes' diffusion path is a well-known approach to provide improved separation efficiencies. This is evident because of the van Deemter equation [109]. The dependence of the third term (*C*-term), is considered to represent mainly the resistance to mass transfer in the mobile phase, on the square of the particle size translates into a large decrease in the plate height with smaller particles, especially at high linear velocities. As demonstrated by Knox, Giddings and others, small particle diameters induce an increase in efficiency, optimal velocity and mass transfer [110–114]. Therefore, efficient separations can be performed with shorter analysis times when sub-2 μm particles are used [115]. However, very fine particles induce a large back pressure (ΔP) according to Darcy's law. The Kozeny–Carman equation describes that flow resistance is directly proportional to the square of particle diameter. Resulting from this, when the linear velocity is increased and the particle diameter is decreased, then it can generate a back pressure higher than 400 bar, even with a column longer than 3 cm. To overcome this problem, providers have commercialized inhomogeneous particle size distribution of 1.8 μm with larger particles packed in the columns [116]. As published by Jorgenson and co-workers [6,7,117], the development of new chromatographic systems compatible with very high pressures (ca. 5000 bar) can overcome this drawback. Theoretically, a 5 cm long column packed with 1.7 μm particles can provide a comparable theoretical plate number with a 15 cm long column packed with 5 μm particles. Higher linear velocities or higher flow rates for a given internal dimension column can be used for smaller particles. As shown in Fig. 4, the optimum linear velocity for 1.7 μm particles is approximately three fold higher than that for 5 μm particles. Considering the relationship between the column length and the optimum linear velocity with the particle size, the separation time (t_R) can be written as:

$$t_R = \frac{(1+k)Nh}{D_m \nu} d_p^2 \tag{9}$$

where *k* is the retention factor, *N* is the plate count, *h* is the reduced plate height, D_m is the analyte diffusion coefficient, ν is the reduced linear velocity and d_p is the particle diameter. It can be seen from Eq. (9) that an efficient way to reduce separation time is to use small particles. Fig. 5 shows separations of five alkylbenzenes by columns with various particle sizes under isocratic conditions [118]. The average resolution for the alkylbenzenes was almost the same for the three columns; however, the separation time was reduced from 15 to 6.6 and to 1.7 min for 5, 3.5, and 1.7 μm particle-packed columns, respectively [118].

The relationship between resolution (*R*), column length (*L*), and particle size (d_p) can be expressed for a given chromatographic condition as:

$$R \propto \sqrt{N} \propto \sqrt{\frac{L}{d_p}} \tag{10}$$

This suggests that a high resolution separation can be achieved by using a relative long column packed with small particles. In this case, both separation time and pressure drop are increased proportionally.

The first commercially available column packed with sub-2 μm particles was the Acquity BEH (1.7 μm) of Waters, released in

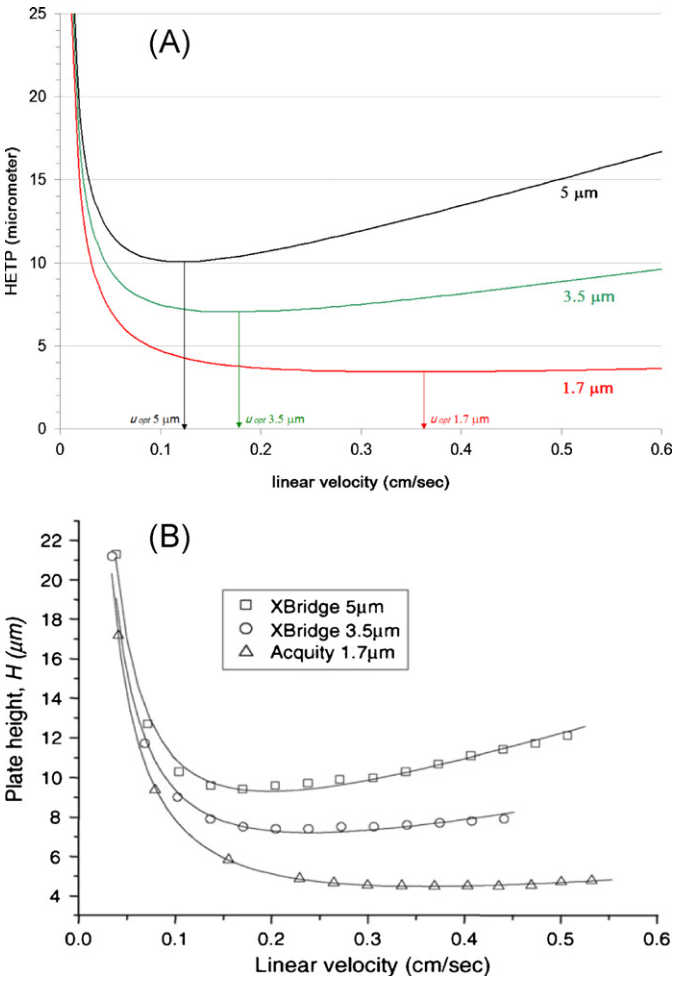

Fig. 4. (A) Theoretical H–u curves of 5 µm, 3.5 µm, and 1.7 µm fully porous particles (molecular weight of 300 g/mol, a reduced plate height minimum of $h = 2$ and same packing quality were assumed) and (B) experimental H–u plots obtained for acetophenone on Acquity and XBridge columns. Columns: Acquity BEH C18, 1.7 µm, 10 cm × 2.1 mm ID; XBridge C18, 3.5 µm, 15 cm × 4.6 mm ID; XBridge C18, 5 µm, 25 cm × 4.6 mm ID.
Panel (B) of this figure was taken from Ref. [12] with permission.

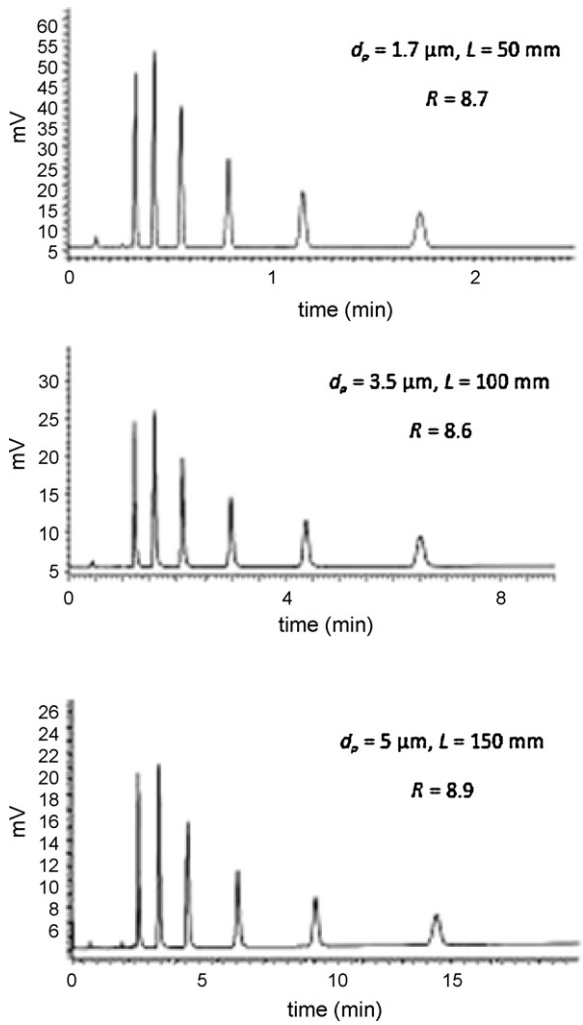

Fig. 5. Experimental chromatograms of alkylbenzenes by columns with various particle sizes (1.7 µm, 3.5 µm and 5 µm) and various lengths (50 mm, 100 mm and 150 mm respectively) under isocratic conditions.
From Ref. [118] with permission.

2004. Now several vendors provide columns packed with sub-2 µm porous particles, the most popular packing beside the Acquity, are the Zorbax RRHD 1.8 µm, Hypersil Gold 1.9 µm and Grace vision HT 1.5 µm. Today the 2 µm and sub-2 µm packings are widespread and applied with great success in different fields of analysis. Table 3 summarizes the recent commercially available 2 µm and sub-2 µm totally porous columns.

Several papers presented the gain in efficiency of sub-2 µm particles compared to 3–5 µm particles [9,12,119–121]. Under conditions of optimal velocity and for the same column length, the 1.7 µm particles provided improved efficiency (N) compared to a 3.5 µm and 5 µm phases [12]. According to a recent study the combination of high optimal flow rates and shorter column lengths allowed a gain in speed by a factor of roughly 4.5 and 3.5 in comparison with 5 µm and 3.5 µm particles, respectively, without sacrificing efficiency. However a slightly higher than expected C-term measured from experimental Knox plots is ascribed to residual temperature effect under non-ideal adiabatic conditions, lower packing efficiency and extra column band broadening [12]. Guillarme et al. presented that applying sub-2 µm particles can make the separation faster with a factor of 3–8 compared to conventional particles [119]. Another study reported an analysis time reduction up to a factor of 12, using small columns packed with sub-2 µm particles compared to a conventional LC separation, without affecting the quality of separation [121]. Please note that the plate height values were not corrected for extra-column band-broadening in these referred papers [12,119–121].

In spite of the several published data and results on the very good efficiency of sub-2 µm particles, the advantage of using smaller particles is not as large as expected. Wirth discussed about the slow mass transport due to analyte desorption from the stationary phase as a possible contribution to the lower than expected efficiency [122].

The higher than expected values of h_{min} for sub-2-µm particles has been a subject of considerable research, which has raised many possible explanations, including heating from higher friction [6,9,123], and radially inhomogeneous packing density [124]. The contribution from friction-induced heating does not explain the higher value of h_{min} for 1.0 µm particles with pressures exceeding 6000 bar [124]. The packing is demonstrated to be inhomogeneous, but even accounting for this still gives an excessively large value of $C_{reduced}$ term [124]. Mobile phase compressibility has recently been shown to have an impact in increasing $C_{reduced}$, in a study where pressure was increased from 2500 to 6300 bar [125], but it has yet not been explored at the much lower pressures of typically <700 bar used in commercial instruments.

Table 3
Commercially available 2 μm and sub-2 μm HPLC columns.

Vendor	Column/product name	Average particle diameter (μm)
Alltech (Grace Davison)	VisionHT	1.5
Shant Laboratories	Pathfinder	1.5
Fortis Technologies	Fortis 1.7	1.7
Orachem Technologies	Emerald, Epitomize	1.7
Phenomenex	Luna, Kinetex	2.0, 1.7
Sepax	GP-8 and GP-18	1.7
Waters	Acquity BEH, CSH	1.7
Agilent Technologies	Zorbax Rapid Resolution HT/HD	1.8
Bischoff	ProntoPEARL TPP Ace-EPS	1.8
ES Industries	Epic Sub-2	1.8
Knauer	BlueOrchid	1.8
Macherey-Nagel	Nucleodur	1.8
MicroSolv Technology	Cogent Diamond & Silica-C	1.8
Micro-Tech Scientific	Microsil	1.8
Perkin Elmer	BrownLee	1.9
Restek	Pinnacle DB/Ultra II	1.9
Thermo	Hypersil Gold	1.9
Varian	Pursuit UPS	1.9
Agela Technologies	Rapid aSB	2.0
Hitachi	LaChromUltra	2.0
Imakt	Presto	2.0
Shiseido	Capcell Pack	2.0
Tosoh Haas	TSKgel SuperODS	2.0
YMC	Ultra-Fast	2.0
Zirchrom	Zirchrom	2.0

Most of the data were taken from Ref. [110].

Guiochon first used a term of heat contribution to the overall reduced HETP of a chromatographic column under very high pressure conditions [126,127]. In this equation HETP is the sum of five main contributions, those due to (1) longitudinal diffusion (the B term); (2) eddy diffusion (the A term); (3) the external film mass transfer resistance (the C_f term); (4) the trans-particle mass transfer resistance (the C_p term); and (5) an additional contribution due to the heat friction of the eluent percolating across the bed, h_{heat}.

$$h = A + \frac{B}{\nu} + C_f\nu + C_p\nu + h_{heat} \quad (11)$$

The fifth term in the reduced HETP equation is needed to account for the band broadening effect of the heat generated by the friction of the eluent percolating through the bed and causing the formation of a radial temperature gradient across the whole column when very high pressure drops are imposed along the column. Because the adsorption constant of the solute is temperature dependent, its migration velocity is a function of the radial position across the column diameter, therefore the concentration profiles of eluting bands can be seriously warped [128]. As any other sources of flow heterogeneity, this term is written under the following form:

$$h_{heat} = \frac{1}{(1/2\lambda_{heat}) + (1/2\omega_{heat}\nu)} \quad (12)$$

where λ_{heat} is the eddy dispersion coefficient related to a flow exchange mechanism generated by heat friction in the column and ω_{heat} is eddy dispersion coefficient related to a diffusion exchange mechanism (Aris) generated by heat friction in the column.

Gritti and Guiochon demonstrated, that the porosity of the particles strongly affects the column efficiency at high flow rates, hence under high pressure conditions. This was clearly proven by the values measured for the reduced HETPs of narrow-bore columns packed with superficially (internal porosity 0.2) and totally (internal porosity 0.4) porous particles [107]. Shell particles suffer less from the negative effects of heat friction, radial temperature gradients, and transverse differential migration velocity than those packed with totally porous particles.

Beside the heat effects of high pressure, the mobile phase density, viscosity, the diffusion coefficients, the equilibrium constants, the retention factors, the efficiency parameters also mainly depend on the pressure. The compressibility of liquids can be considered as constant at constant temperature in the range of pressures used in conventional HPLC (below 400 bar), at least as far as the column flow rate and the pressure gradient along the column are concerned. However, above 400 bar, the compressibility does depend on the pressure. Up to several kbar, the pressure dependence of the volume, occupied by a given mass of liquid is well accounted for Tait equation [129]. At 1000 bar the specific volume of common solvents decreases to approximately 90–98%, at 2500 bar to 84–93% than it is at atmospheric pressure [130]. The viscosity of liquids increases with increasing pressure. In the pressure range up to a few kbar, this variation is nearly linear. At 1000 bar the viscosity of organic solvents increases by a factor of 1.4–2 than it is at atmospheric pressure [130,131].

Most investigations of the effects of pressure on retention data in HPLC were obtained at relatively low pressures, i.e., 50–300 bar. The results of measurements by Rogers and co-workers [132–134] at pressures up to 3500 bar showed that changes in the retention factors can exceed 300% and that they are accompanied by shifts in the elution orders.

Summing up the effects of ultra high pressure (mainly the heat friction and the change in diffusion coefficients), they can cause a loss in efficiency compared to the previously expected efficiency of sub-2 μm particles. Table 4 summarizes the minimum reduced plate height values, minimum plate heights and the maximum plate count of the columns packed with totally porous particles, reported in recent papers. It can be seen that there are a serious deviation among the h_{min} data of sub-2 μm particles reported in different papers. The 1.5 μm Grace Vision HT column (5 cm × 2.0 mm) can achieve plate heights between 7200 and 11,000. The 5 cm long, narrow bore 1.7 μm Acquity BEH columns provide reduced plate height minimum values in the range of h_{min} = 2.3–3.8, while 10–15 cm long Acquity BEH columns give h_{min} = 2.0–2.9 values. The 1.8 μm Zorbax narrow bore 5 cm long columns perform h_{min} = 2.5–3.8. Columns packed with 1.9 μm porous particles (Restek Pinnacle and Hypersil Gold) provide h_{min} = 2.6–3.7 values while the 2 μm particles (YMC UltraHT Pro) packed in 5 cm long narrow bore columns give reduced plate height values around $h_{min} \sim 2.5$.

A systematic evaluation was showed in which several h_{min} and $HETP_{min}$ data of 5 cm long narrow bore columns were reported [13]. All the data were corrected for extra-column band broadening, the same test analyte and mobile phase was used in that study for evaluating the columns of different manufacturers'. In Fig. 6 plots of h_{min} and $HETP_{min}$ data against particle diameter are presented on the basis of previously reported data [13]. Fig. 6 obviously shows that the efficiency of sub-2 μm particles is not as high as it was theoretically predicted earlier. The difference between the theoretical and experimental column efficiency increases as the particle size is reduced. In spite of the $HETP_{min}$ values are smaller on smaller particles, the smaller the particle size the higher the obtained reduced plate height minimum value is. The 3 μm particles provide h_{min} value close to 2, while the 1.5 μm particles achieve $h_{min} \sim 2.9$.

As a conclusion, the possible adverse heat effects and inhomogenous packing density of narrow bore columns packed with very fine particles (d_p < 2 μm), provide a compromised efficiency of recent small columns. Summing up these effects the overall efficiency of small narrow bore columns packed with different size very fine particles (in the size range of d_p = 1.5–2.1 μm) is nearly the same [13]. Fekete et al. showed that 1.7 μm Waters Acquity BEH C18, 1.9 μm Restek Pinnacle C18 and 2.1 μm Fortis C18 columns gave the same efficiency and separation speed when 5 cm long narrow bore columns were applied for the separation of steroids [13].

Table 4
Summary of reported minimum reduced plate height values, minimum plate height values and maximum plate numbers obtained with different fully porous fine particles packing.

Stationary phase	Column dimension	h_{min}	H_{min} (μm)	N_{max}	Solute	Reference
1.5 μm Grace Vision HT C18	2.0 mm × 50 mm	3.1	4.6	10,870	Ethinylestradiol	[13]
	2.0 mm × 50 mm	3.1	4.6	10,870	Bicalutamide	[13]
	2.0 mm × 50 mm	4.6	6.9	7246	Ivermectin	[13]
1.7 μm BEH C18	2.1 mm × 50 mm	2.6	4.4	11,364	Butyrophenone	[139]
	2.1 mm × 50 mm	3.3	5.6	8990	Acenaphthene	[136]
	2.1 mm × 50 mm	2.8	4.8	10,500	Butylparaben	[120]
	2.1 mm × 50 mm	2.8	4.7	10,638	Ethinylestradiol	[13]
	2.1 mm × 50 mm	2.8	4.8	10,417	Bicalutamide	[13]
	2.1 mm × 50 mm	3.8	6.5	7692	Ivermectin	[13]
	2.1 mm × 100 mm	2.9	4.9	20,408	Phenol	[142]
	2.1 mm × 100 mm	2.5	4.2	23,810	Propylparaben	[142]
	2.1 mm × 150 mm	2	3.4	44,118	Naphtho[2,3-a]pyrene	[98]
1.7 μm BEH Shield RP18	2.1 mm × 50 mm	2.3	3.9	12,800	Butylparaben	[120]
1.8 μm Zorbax Eclipse XDB C18	2.1 mm × 50 mm	3	5.4	9300	Butylparaben	[120]
1.8 μm Zorbax Extend C18	2.1 mm × 50 mm	2.5	4.5	11,100	Butylparaben	[120]
1.8 μm Zorbax Stable Bond C18	2.1 mm × 50 mm	3.2	5.8	8700	Butylparaben	[120]
	2.1 mm × 50 mm	2.8	4.8	10,417	Ethinylestradiol	[13]
	2.1 mm × 50 mm	2.72	4.9	10,204	Bicalutamide	[13]
	2.1 mm × 50 mm	3.8	6.9	7246	Ivermectin	[13]
1.9 μm Hypersil GOLD C18	2.1 mm × 50 mm	2.6	4.9	10,100	Butylparaben	[120]
	2.1 mm × 50 mm	3.7	7.1	7042	Ivermectin	[13]
1.9 μm Restek Pinnacle DB C18	2.1 mm × 50 mm	2.9	4.9	10,204	Ethinylestradiol	[13]
	2.1 mm × 50 mm	2.6	4.9	10,204	Bicalutamide	[13]
	2.1 mm × 50 mm	3.2	6.1	8197	Ivermectin	[13]
2.0 μm YMC UltraHT Pro C18	2.0 mm × 50 mm	2.5	5.0	10,000	Ethinylestradiol	[13]
	2.0 mm × 50 mm	2.5	5.0	10,000	Bicalutamide	[13]

6. Instrumentation, extra-column effects

Each serious progress in column technology requires important progress in instrument design and manufacturing [135]. Extra-column band spreading affects the measured performance of columns packed with small particles, especially for columns with an internal diameter smaller than the classical standard of 4.6 mm [136]. Recently several papers focused on the extra-column effect as a major factor that negatively impacts the apparent performance of columns packed with core–shell or sub-2 μm particles [15,16,135,136]. Conventional high performance liquid chromatographic (HPLC) systems contribute to the measured peak variance approximately 40–200 μL^2 [121,135] while standard ultra performance or ultra-high pressure chromatographic systems have a

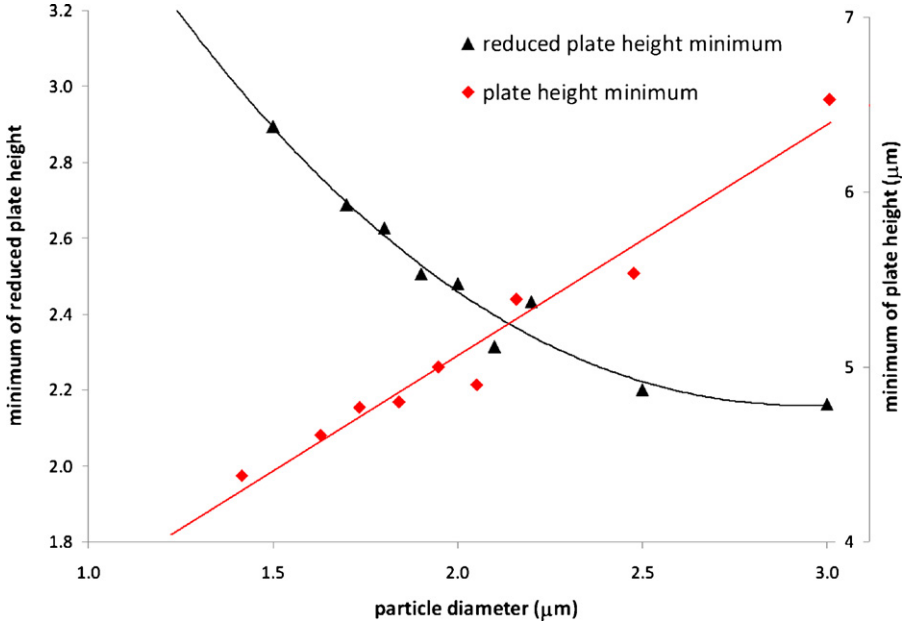

Fig. 6. $HETP_{min}$ and h_{min} data against particle diameter. Test analyte: ethinyl-estradiol (MW = 296 g/mol). Experiments were conducted on a 5 cm long narrow bore columns in 48/52 acetonitrile/water, η = 0.85 cP, at 35 °C. Injected volume: 0.5 μL, system: Waters Acquity UPLC. The plate heights were corrected for extracolumn peak broadening. Columns: Grace Vision HT 1.5 μm (50 mm × 2.0 mm), Waters UPLC BEH C18 1.7 μm (50 mm × 2.1 mm), Zorbax SB C18 1.8 μm (50 mm × 2.1 mm), Restek Pinnacle DB C18 1.9 μm (50 mm × 2.1 mm), YMC UltraHT Pro C18 2.0 μm (50 mm × 2.0 mm), Fortis C18(2) 2.1 μm (50 mm × 2.1 mm), Shim-pack XR-ODS-2 2.2 μm (50 mm × 2.0 mm), Phenomenex Luna C18(2)-HST 2.5 μm (50 mm × 2.0 mm) and Thermo Hypersil ODS 3.0 μm (50 mm × 2.1 mm).

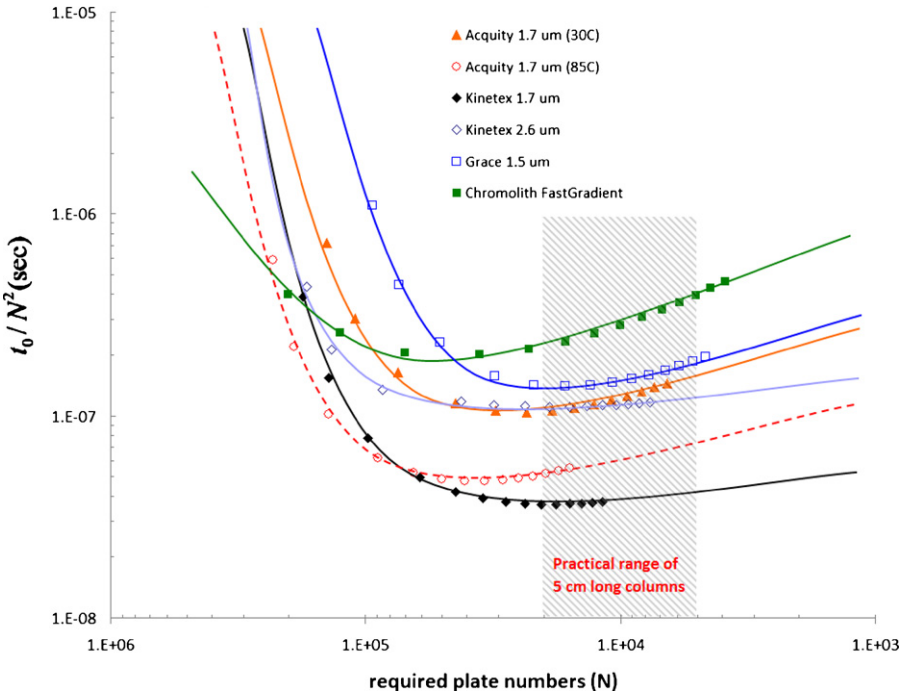

Fig. 7. t_0/N^2 versus N plots of estradiol (272 g/mol). Experiments were conducted on a 5 cm long narrow bore columns in 48/52 acetonitrile/water, $\eta = 0.85$ cP, at 35 °C. Available max. pressure: 200 bar for the Chromolith column, 600 bar for Kinetex columns, 830 bar for Grace Vision HT column and 1000 bar for Waters BEH column. Injected volume: 0.5 μL, system: Waters Acquity UPLC. The plate heights were corrected for extra-column peak broadening, column permeability data were corrected with system pressure drop.

contribution typically in the range of 4–9 μL^2 [15,16,121,135–137]. In the case of very efficient columns, the extra-column variance of the commercially available LC systems with very low dispersion (<10 μL^2) is not negligible. A recent study showed that, when a 5 cm × 2.1 mm, 1,7 μm Kinetex column is used, only the 60–90% of the real intrinsic column efficiency can be realized with very low dispersion UHPLC instruments (k was varied between $k = 1.5$ and $k = 5$, small polar neutral test analyte having a molecular weight of 272 g/mol was used) [138]. Further optimizing in UHPLC systems such as using smaller volume needle seat capillary, narrower and shorter connector capillary tubes and a smaller volume detector cell can provide a significant decrease in extra-column contribution down to around 1–5 μL^2 [45,135]. With these improvements the efficiency loss can be significantly reduced [135].

7. The achievable analysis speed with very efficient small columns; a comparison of recent possibilities

In this section the kinetic efficiency of recent very efficient 5 cm long narrow bore columns are compared by means of their kinetic plots. Kinetic plots were reconstructed on the basis of a systematic evaluation.

The kinetic efficiency (H–u curves) of 5 cm long narrow bore columns packed with fully porous and core–shell particles was determined earlier and reported in previous papers [15,16]. The kinetic efficiency of the columns was determined with a mobile phase composition, which gave a range of retention factors (k) between 3.4 and 6.6 both for the small molecular weight test analyte (272 g/mol) and for a polypeptide (4.1 kDa). Differences in the retention factors (k) of course affect the shape of the obtained van Deemter type curves, as both the B- and C-terms of the equations, depend on analyte retention. We have not made attempt to adjust the mobile phase composition to guarantee constant k for all analytes, because this would introduce additional variability in terms of viscosity and analyte diffusion coefficients, which would outweigh the minor effect of retention.

Fig. 7 shows the calculated isocratic kinetic plots (t_0/N^2 versus N) of estradiol (272 g/mol) on the compared columns at the maximum applicable pressure for each column to represent the utilization of maximum performance. The data for maximum pressure were obtained from the column manufacturers: 1000 bar for Waters Acquity BEH, 830 bar for Grace Vision HT columns, 600 bar for Kinetex columns and 200 bar for the Chromolith column. These plots represent the theoretical separation speed when the maximum performance of an UHPLC system is utilized. The resulting curves, one for each column, demonstrate the maximum speed obtainable at a given required plate number (N) and also demonstrate the effect of the choice of column (stationary phase type; totally porous particles, shell particles, monolith column). Please note that the plate times depend on the maximum allowable pressure drop, which is different for the tested columns. A column can offer faster separation if it has a stationary phase with stronger mechanical stability than the column which has lower mechanical stability.

The experimental kinetic plots show that the 1.7 μm core–shell packing (Kinetex) provides the most favourable plate time values and offers the shortest analysis time in the practical range of short columns (if the separation requires 5–20,000 plate counts). The second choice in this plate number range is the Waters BEH column (fully porous hybrid particles) when it is used at elevated temperature ($T = 85$ °C). The 2.6 μm Kinetex column (core–shell particles) performs similar separation speed as the columns packed with sub-2 μm totally porous particles. In the plate number range of small columns the monolith column provides the slowest separation, however it is necessary to mention that the monolithic column is the most beneficial when very high plate counts are required for a given separation ($N > 200{,}000$).

We can conclude that in the case of small analytes, the sub-2 μm core–shell packing (Kinetex) offers the chance of the fastest separation, while the sub-3 μm core–shell column performs similar

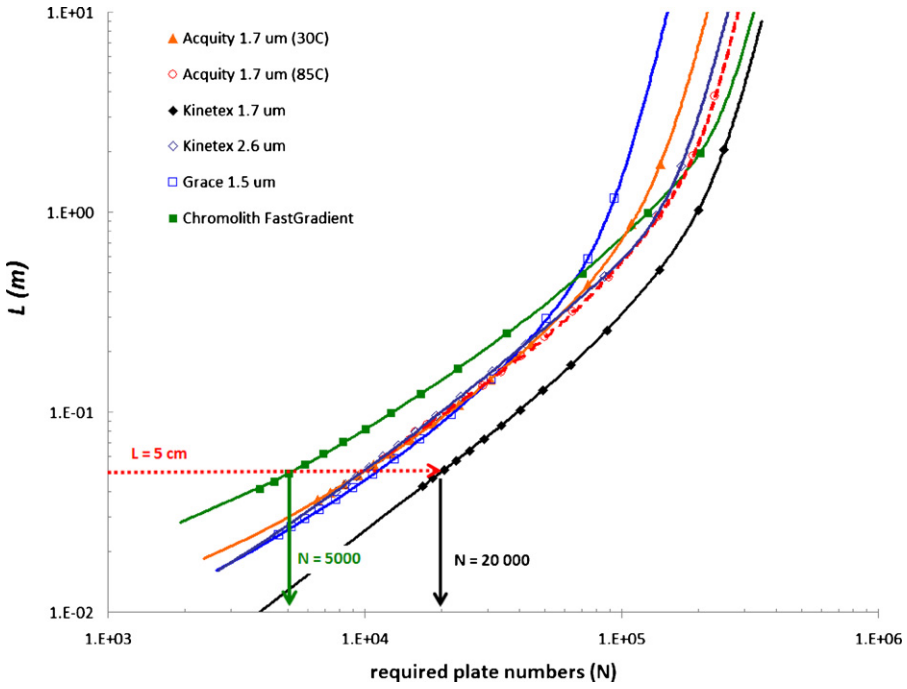

Fig. 8. Column length (m) versus plate numbers plots of estradiol (272 g/mol). Experiments were conducted on 5 cm long narrow bore columns in 48/52 acetonitrile/water, η = 0.85 cP, at 35 °C. Available max. pressure: 200 bar for the mChromolith column, 600 bar for Kinetex columns, 830 bar for Grace Vision HT column and 1000 bar for Waters BEH column. Injected volume: 0.5 μL, system: Waters Acquity UPLC. The plate heights were corrected for extra-column peak broadening, column permeability data were corrected with system pressure drop.

separation speed as the columns packed with sub-2 μm fully porous particles. Increasing the separation temperature can significantly shorten the separation speed. Thermally stable sub-2 μm totally porous particles can offer comparable separation speed at high temperature (T = 85 °C) as the sub-2 μm core–shell particles at ambient temperature (T = 20–35 °C). Consequently a column can offer faster separation if it has higher thermal stability than the column which has lower thermal stability. The obtainable maximum

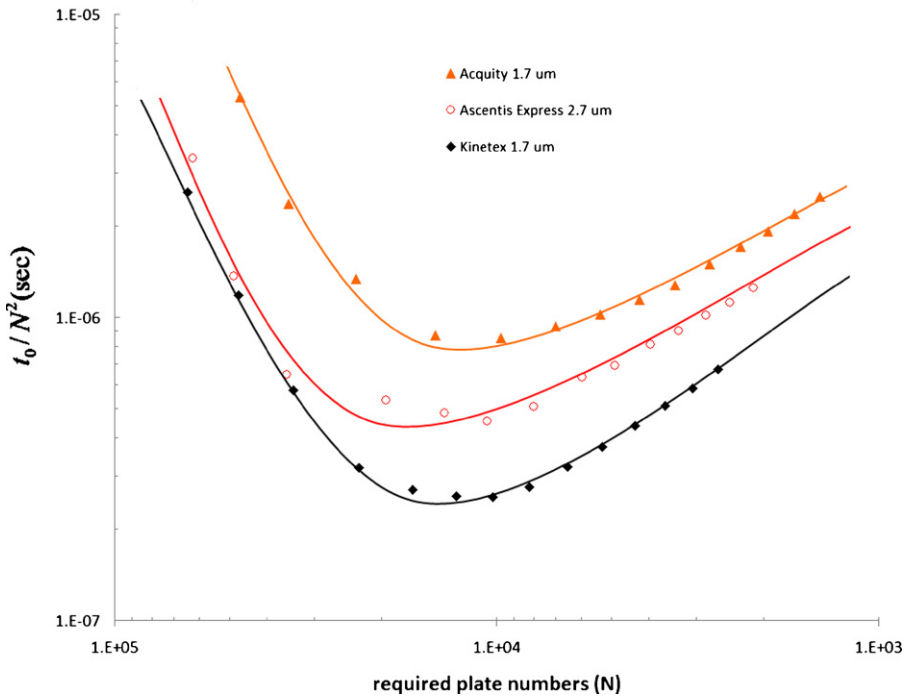

Fig. 9. t_0/N^2 versus N plots of a 4.1-kDa polypeptide. Experiments were conducted on 5 cm long narrow bore columns in acetonitrile/water/TFA 140/860/1, η = 0.99 cP, at 35 °C. Available max. pressure: 600 bar for Ascentis Express and Kinetex 1.7 μm columns and 1000 bar for Waters BEH column. Injected volume: 0.5 μL, system: Waters Acquity UPLC. The plate heights were corrected for extra-column peak broadening, column permeability data were corrected with system pressure drop.

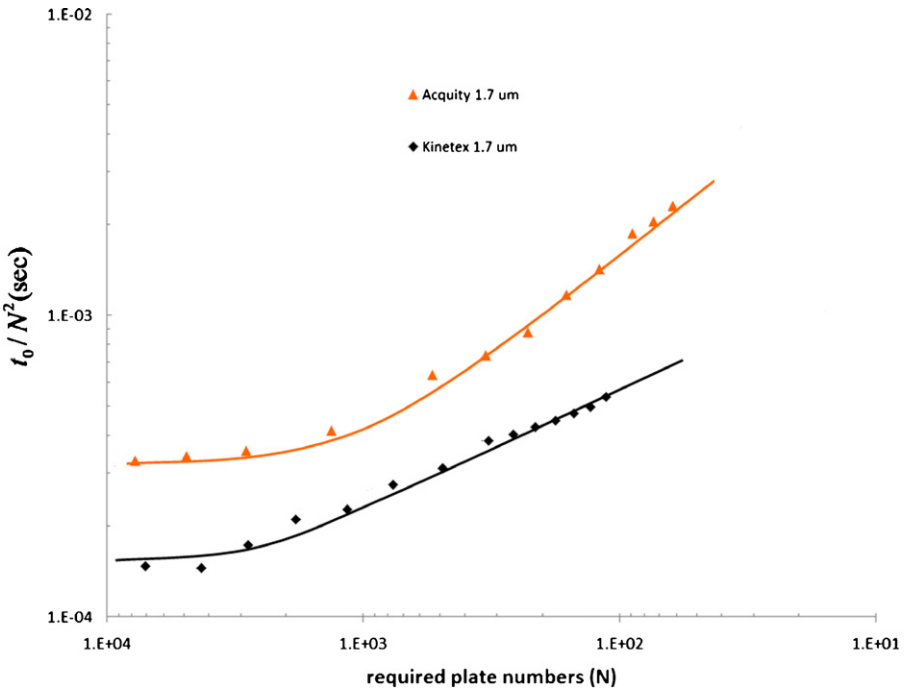

Fig. 10. t_0/N^2 versus N plots of a 39-kDa protein. Experiments were conducted on 5 cm long narrow bore columns in acetonitrile/water/TFA 450/550/1, η = 0.99 cP, at 35 °C. Available max. pressure: 600 bar for Kinetex 1.7 μm column and 1000 bar for Waters BEH column. Injected volume: 0.5 μL, system: Waters Acquity UPLC.

separation speed depends not only on the obtained plate numbers and column permeability but on the mechanical and thermal stability.

Another representation of kinetic plots (column length versus plate counts) can be seen in Fig. 8. These curves demonstrate that similar quality in separation can be performed with approximately the same length of sub-2 μm totally porous and sub-3 μm core–shell particles, while the same quality of separation can be achieved with significantly shorter 1.7 μm Kinetex column. Therefore the expected analysis speed is the shortest when the 1.7 μm Kinetex column is applied.

While the benefit of core–shell particles is evident with small molecules, the improvement is most significant with peptide and protein molecules. Figs. 9 and 10 show the experimental isocratic kinetic plots (t_0/N^2 versus N) of a 4.1 kDa polypeptide and a 39-kDa protein on the compared columns at the maximum applicable pressure for each column. The data for maximum pressure were obtained from the column manufacturers: 1000 bar for Waters BEH, and 600 bar for Kinetex and Ascentis Express columns.

The experimental kinetic plots of the 4.1 kDa polypeptide (Fig. 9) obviously show that decreasing the shell thickness manifests in fastest separation when peptides are separated. The 1.7 μm core–shell packing (Kinetex, 0.23 μm porous silica layer) provides the most efficient separation and offers the shortest analysis time in the range of N = 1000–100,000. While the packing of Ascentis Express (0.5 μm porous silica layer) performs less efficient separation than the Kinetex 1.7 μm material but offers significantly faster analysis than the fully porous sub-2 μm packing.

Fig. 10 shows a similar tendency as Fig. 9 for a 39-kDa protein. Packing of core–shell and fully porous material of the same particle diameter (1.7 μm) are compared in this example. Fig. 10 obviously proves the benefit of core–shell particles for the separation of large analytes. The core–shell packing offers about two times faster separation than the fully porous particle of the same size when the 39-kDa protein is analysed.

We can conclude that recent small columns with core–shell packing can provide faster separations than the columns of same size packed with fully porous particles for both small and macromolecules.

8. Conclusion

This review presents the possibilities of recent very efficient columns in fast liquid chromatographic separations. Among the fast LC techniques, sub-2 μm and core–shell particles are the most popular and widespread ones today.

The 5 cm long narrow bore columns packed with fully porous particles can achieve plate counts between N = 7000–13,000 while the 5 cm long columns with core–shell packing can provide plate numbers around N = 9–19,000 for small analytes. While the benefit of core–shell particles is evident with small molecules, the improvement is most significant with peptide and protein molecules. We can conclude that recent small columns with core–shell packing can provide faster separations than the columns of same size packing with fully porous particles for both small and macromolecules. The 5 cm long, narrow bore 1.7 μm Kinetex C18 column provides approximately 50% improvement in plate heights for separation of peptides in comparison with fully porous particles. Reducing the particle size from 2.6 μm to 1.7 μm manifests in 20% improvement in plate heights and optimum linear velocity shifts towards higher values. Recently the most efficient commercially available packing is the core–shell type Kinetex. Another promising packing is the new 1.7 μm Eiroshell.

These very efficient small columns perform really high plate numbers however the efficiency of narrow bore columns is compromised. The obvious correlation between the loss in efficiency and decrease of column diameter cause that narrow bore short columns provide not always the faster separation than standard bore columns especially when the separation requires small plate counts.

The possible adverse heat effects and inhomogeneous packing density of narrow bore columns packed with very fine particles (d_p < 2 μm), provide a compromised efficiency of recent small columns. Summing up the adverse effect of very high pressure the

overall efficiency of small narrow bore columns packed with different size very fine particles in the size range of d_p = 1.5–2.1 μm are practically the same.

Extra-column band spreading also affects the measured performance (apparent plate number) of columns packed with small particles, especially for short columns with an internal diameter smaller than the classical standard of 4.6 mm. In the case of very efficient small columns, the extra-column variance of the commercially available LC systems with very low dispersion (<10 μL^2) is not negligible. Today it is not possible to utilize the potential of these very efficient small columns.

References

[1] J. Zweigenbaum, K. Heinig, S. Steinborner, T. Wachs, J. Henion, Anal. Chem. 71 (1999) 2294.
[2] K. Yu, M. Balogh, LC–GC N. Am. 19 (2001) 60.
[3] T. Wehr, LC–GC N. Am. 20 (2002) 954.
[4] S. Fekete, K. Ganzler, J. Fekete, J. Pharm. Biomed. Anal. 49 (2009) 830.
[5] J.H. Knox, M. Saleem, J. Chromatogr. Sci. 7 (1969) 614.
[6] J.E. MacNair, K.C. Lewis, J.W. Jorgenson, Anal. Chem. 69 (1997) 983.
[7] J.E. MacNair, K.D. Patel, J.W. Jorgenson, Anal. Chem. 71 (1999) 700.
[8] N. Wu, J.A. Lippert, M.L. Lee, J. Chromatogr. A 911 (2001) 1.
[9] A. de Villiers, H. Lauer, R. Szucs, S. Goodall, P. Sandra, J. Chromatogr. A 1113 (2) (2006) 84.
[10] F. Gritti, G. Guiochon, J. Chromatogr. A 1138 (2007) 141.
[11] F. Gritti, G. Guiochon, Anal. Chem. 80 (2008) 5009.
[12] A. de Villiers, F. Lestremau, R. Szucs, S. Gélébart, F. David, P. Sandra, J. Chromatogr. A 1127 (2006) 60.
[13] S. Fekete, K. Ganzler, J. Fekete, J. Pharm. Biomed. Anal. 51 (2010) 56.
[14] D.J. Phillips, M. Capparella, U.D. Neue, Z. El Fallah, J. Pharm. Biomed. Anal. 15 (1997) 1389.
[15] E. Oláh, S. Fekete, J. Fekete, K. Ganzler, J. Chromatogr. A 1217 (2010) 3642.
[16] S. Fekete, K. Ganzler, J. Fekete, J. Pharm. Biomed. Anal. 54 (2011) 482.
[17] A.A. Mohammad, R. Panagiota, A. Vincent, W. Naijun, J. Sep. Sci. 31 (2008) 2167.
[18] G.D. Vaijanath, P.K. Pravin, P.R. Pilla, K. Ashok, J. Pharm. Biomed. Anal. 46 (2008) 236.
[19] R. Toporisic, A. Mlakar, J. Hvala, I. Prislan, L. Zupancic-Kralj, J. Pharm. Biomed. Anal. 52 (2010) 294.
[20] B.H. Prasad, W.L. Hae, L. Mi-sun, K. Eun-Hee, K. Sung-Doo, P. Jeonghyeon, L. Miran, H. Sung-Kyu, Y. Young-Ran, J. Chromatogr. B 878 (2010) 1718.
[21] H.K. Mayer, G. Fiechter, E. Fischer, J. Chromatogr. A 1217 (2010) 3251.
[22] .S. Sachin, I.A. Najar, S.C. Sharma, M.K. Verma, M.V. Reddy, R. Anand, R.K. Khajuria, S. Koul, R.K. Johri, J. Chromatogr. B 878 (2010) 823.
[23] L. Hong, D. Zhenxia, Y. Qipeng, J. Chromatogr. B 877 (2009) 4159.
[24] S. Fekete, K. Ganzler, J. Fekete, J. Pharm. Biomed. Anal. 51 (2009) 56.
[25] Y.S. Li, B. Li, N.Y. Han, B.J. Xu, J. Chromatogr. A 1021 (2003) 183.
[26] F. Ai, L. Li, S.-C. Ng, T.T.Y. Tan, J. Chromatogr. A 1217 (2010) 7502.
[27] J.S. Mellors, J.W. Jorgenson, Anal. Chem. 76 (2004) 5441.
[28] C. Thoelen, J. Paul, I.F.J. Vankelecom, P.A. Jacobs, Tetrahedron-Asymmetry 11 (2000) 4819.
[29] J.J. Kirkland, J. Chromatogr. Sci. 38 (2000) 535.
[30] T.J. Barder, P.J. Wohlman, C. Thrall, P.D. DuBois, LC–GC 15 (1997) 918.
[31] N. Wu, D.C. Collins, J.A. Lippert, Y. Xiang, M.L. Lee, J. Microcol. Sep. 12 (2000) 462.
[32] N. Wu, A.J. Lippert, M.L. Lee, J. Chromatogr. A 911 (2001) 1.
[33] K. Rissler, J. Chromatogr. A 1131 (2006) 142.
[34] N. Wu, Y. Liu, M.L. Lee, J. Chromatogr. A 1131 (2006) 142.
[35] T. Issaeva, A. Kourganov, K. Unger, J. Chromatogr. A 846 (1999) 13.
[36] R.M. Seifar, J.C. Kraak, W.Th. Kok, H. Poppe, J. Chromatogr. A 808 (1998) 71.
[37] J.H. Knox, Anal. Chem. 38 (1966) 253.
[38] C. Horvath, B.A. Preiss, S.R. Lipsky, Anal. Chem. 39 (1967) 1422.
[39] C. Horvath, S.R. Lipsky, J. Chromatogr. Sci. 7 (1969) 109.
[40] J.J. Kirkland, Anal. Chem. 41 (1969) 218.
[41] J.J. Kirkland, F.A. Truszkowski, C.H. Dilks Jr., G.S. Engel, J. Chromatogr. A 890 (2000) 3.
[42] F. Gritti, G. Guiochon, J. Chromatogr. A 1166 (2007) 30.
[43] S. Fekete, J. Fekete, K. Ganzler, J. Pharm. Biomed. Anal. 49 (2009) 64.
[44] F. Gritti, G. Guiochon, J. Chromatogr. A 1218 (2011) 907.
[45] J.O. Omamogho, J.P. Hanrahan, J. Tobin, J.D. Glennon, J. Chromatogr. A 1218 (2011) 1942.
[46] G. Guiochon, F. Gritti, J. Chromatogr. A 1218 (2011) 1915.
[47] D. Cabooter, A. Fanigliulo, G. Bellazzi, B. Allieri, A. Rottigni, G. Desmet, J. Chromatogr. A 1217 (2010) 7074.
[48] J.A. Blackwell, P.W. Carr, J. Liquid Chromatogr. 14 (1991) 2875.
[49] C. Zhu, D.M. Goodall, S.A.C. Wren, LC–GC N. Am. 23 (2005) 1.
[50] H.A. Claessens, M.A. van Straten, Reduction of Analysis Times in HPLC at Elevated Column Temperatures, Eindhoven University of Technology, 2004.
[51] P.T. Jackson, P.W. Carr, Chemtech 28 (1988) 29.
[52] R.J. Maggs, in: A. Zlatkis (Ed.), Advances in Chromatgraphy, Preston, Evanston, IL, 1969, p. 303.
[53] F.D. Antia, C.S. Horvath, J. Chromatogr. 435 (1988) 1.
[54] H. Chen, Cs. Horváth, J. Chromatogr. 705 (1995) 3.
[55] T. Greibrokk, T. Andersen, J. Chromatogr. A 1000 (2003) 743.
[56] S.M. Fields, C.Q. Ye, D.D. Zhang, B.R. Branch, X.J. Zhang, N. Okafe, J. Chromatogr. A 913 (2001) 197.
[57] T. Teutenberg, H.-J. Goetze, J. Tuerk, J. Ploeger, T.K. Kiffmeyer, K.G. Schmidt, W.gr. Kohorst, T. Rohe, H.-D. Jansen, H. Weber, J. Chromatogr. A 1114 (2006) 89.
[58] S. Heinisch, J.L. Rocca, J. Chromatogr. A 1216 (2009) 642.
[59] C. Stella, S. Rudaz, J.-L. Veuthey, A. Tchapla, Chromatographia 53 (2001) 113.
[60] Y. Yang, LC–GC Europe 6 (2003) 37.
[61] J. Nawrocki, C. Dunlap, A. McCornnich, P.W. Carr, I. Pert, J. Chromatogr. A 1028 (2004) 1.
[62] J. Nawrocki, C. Dunlap, J. Li, J. Zhao, C.V. McNeff, A. McCormick, P.W. Carr, I.I. Part, J. Chromatogr. A 1028 (2004) 31.
[63] C.Mc. Neff, L. Zigan, K. Johnson, P.W. Carr, A. Wang, A.M. Weber-Main, LC–GC 18 (2000) 514.
[64] G. Vanhoenacker, A. Dos Santos Pereira, T. Kotsuka, D. Cabooter, G. Desmet, P. Sandra, J. Chromatogr. A 1217 (2010) 3217.
[65] S. Louw, F. Lynen, M. Hanna-Brown, P. Sandra, J. Chromatogr. A 1217 (2010) 514.
[66] K. Im, H. Park, S. Lee, T. Chang, J. Chromatogr. A 1216 (2009) 4606.
[67] H.G. Gika, G. Theodoridis, J. Extance, A.M. Edge, I.D. Wilson, J. Chromatogr. B 871 (2008) 279.
[68] R. Berta, M. Babják, M. Gazdag, J. Pharm. Biomed. Anal. 54 (2011) 458.
[69] N. Tanaka, H. Kobayashi, N. Ishizuka, H. Minakuchi, K. Nakanishi, K. Hosoya, T. Ikegami, J. Chromatogr. A 965 (2002) 35.
[70] N. Wu, J. Dempsey, P.M. Yehl, A. Dovletoglou, D.K. Ellison, J.M. Wyvratt, Anal. Chim. Acta 523 (2004) 149.
[71] S. Hjertén, J-L. Liao, R. Zhang, J. Chromatogr. 473 (1989) 273.
[72] L. Nováková, L. Matysová, D. Solichová, M.A. Koupparis, P. Solich, J. Chromatogr. B 813 (2004) 191.
[73] M. Cledara-Castro, A. Santos-Montes, R. Izquierdo-Hornillos, J. Chromatogr. A 1087 (2005) 57.
[74] K.S. Mriziq, J.A. Abia, Y. Lee, G. Guiochon, J. Chromatogr. A 1193 (2008) 97.
[75] H. Minakuchi, K. Nakanishi, N. Soga, N. Ishizuka, N. Tanaka, J. Chromatogr. 797 (1998) 121.
[76] F. Gritti, G. Guiochon, J. Chromatogr. A 1216 (2009) 4752.
[77] H. Minakuchi, K. Nakanishi, N. Soga, N. Ishizuka, N. Tanaka, J. Chromatogr. A 762 (1997) 135.
[78] R. Skudas, B.A. Grimes, M. Thommes, K.K. Unger, J. Chromatogr. A 1216 (2009) 2625.
[79] S. Eeltik, P. Gzil, W.Th. Kok, P.J. Schoenmakers, G. Desmet, J. Chromatogr. A 1130 (2006) 108.
[80] K. Miyabe, J. Chromatogr. A 1183 (2008) 49.
[81] G. Guiochon, J. Chromatogr. A 1168 (2007) 101.
[82] R. Wu, L. Hu, F. Wang, M. Ye, H. Zou, J. Chromatogr. 1184 (2008) 369.
[83] D. Wistuba, J. Chromatogr. A 1217 (2010) 941.
[84] J. Randon, S. Huguet, A. Piram, G. Puy, C. Demesmay, J.-L. Rocca, J. Chromatogr. A 1109 (2006) 19.
[85] J. Randon, S. Huguet, C. Demesmay, A. Berthod, J. Chromatogr. A 12317 (2010) 1496.
[86] P. Jandera, J. Urban, V. Skeriková, P. Langmaier, R. Kubicková, J. Planeta, J. Chromatogr. 1217 (2010) 22.
[87] Y. Lv, D. Mei, X. Pan, T. Tan, J. Chromatogr. B 878 (2010) 2461.
[88] T.J. Causon, A. Nordborg, R.A. Shellie, E.F. Hilder, J. Chromatogr. 1217 (2010) 3519.
[89] G. Desmet, D. Clicq, P. Gzil, Anal. Chem. 77 (2005) 4058.
[90] H. Chen, C. Horvath, J. Chromatogr. A 705 (1995) 3.
[91] K. Kaczmarski, G. Guiochon, Anal. Chem. 79 (2007) 4648.
[92] J. Giddings, Dynamics of Chromatography, Marcel Dekker, New York, NY, 1965.
[93] F. Gritti, G. Guiochon, AIChE J., AICHE-09-11893.
[94] G. Guiochon, A. Felinger, A. Katti, D. Shirazi, Fundamentals of Preparative and Nonlinear Chromatography, 2nd ed., Academic Press, Boston, MA, 2006.
[95] G. Desmet, S. Deridder, J. Chromatogr. A 1218 (2011) 32.
[96] S. Deridder, G. Desmet, J. Chromatogr. A 1218 (2011) 46.
[97] G. Desmet, K. Broeckhoven, J. De Smet, S. Deridder, G.V. Baron, P. Gzil, J. Chromatogr. A 1188 (2008) 171.
[98] F. Gritti, G. Guiochon, J. Chromatogr. A 1217 (2010) 5069.
[99] F. Gritti, G. Guiochon, J. Chromatogr. A 1218 (2011) 1592.
[100] B.G. Yew, J. Ureta, R.A. Shalliker, E.C. Drumm, G. Guiochon, AIChE J. 49 (2003) 642.
[101] J.J. DeStefano, T.J. Langlois, J.J. Kirkland, J. Chromatogr. Sci. 46 (2008) 254.
[102] F. Gritti, I. Leonardis, J. Abia, G. Guiochon, J. Chromatogr. A 1217 (2010) 3819.
[103] F. Gritti, A. Cavazzini, N. Marchetti, G. Guiochon, J. Chromatogr. A 1157 (2007) 289.
[104] F. Gritti, G. Guiochon, J. Chromatogr. A 1217 (2010) 5137.
[105] K. Miyabe, Y. Kawaguchi, G. Guiochon, J. Chromatogr. A 1217 (2010) 3053.
[106] E. Wilson, C. Geankoplis, J. Ind. Eng. Chem. (Fundam.) 5 (1966) 9.
[107] F. Gritti, G. Guiochon, Chem. Eng. Sci. 65 (2010) 6310.
[108] I. Halasz, R. Endele, J. Asshauer, J. Chromatogr. 12 (1975) 37.
[109] J.J. van Deemter, F.J. Zuiderweg, A. Klinkenberg, Chem. Eng. Sci. 5 (1956) 271.

[110] R.E. Majors, Continuing Innovations in Reversed-phase HPLC Column Technology, Pittcon, 2010.
[111] M. Martin, C. Eon, G. Guiochon, J. Chromatogr. 99 (1974) 357.
[112] J.C. Giddings, Anal. Chem. 37 (1965) 60.
[113] J.H. Knox, J. Chromatogr. Sci. 15 (1977) 352.
[114] H. Poppe, J. Chromatogr. A 778 (1997) 3.
[115] R.E. Majors, LC–GC N. Am. 23 (2005) 1248.
[116] B. Barber, J. Henderson, M. Joseph, Poster presented at HPLC 2005, Stockholm, Sweden, 2005 June, 2005.
[117] L. Tolley, J.W. Jorgenson, M.A. Moseley, Anal. Chem. 73 (2001) 2985.
[118] N. Wu, A. Clausen, L. Wright, K. Vogel, F. Bernardoni, Fast UHPLC Using Sub-2 μm Particles and Elevated Pressures for Pharmaceutical Process Development, American Pharmaceutical Review, 2009.
[119] D. Guillarme, D.T.T. Nguyen, S. Rudaz, J.L. Veuthey, J. Chromatogr. A 1149 (2007) 20.
[120] D.T.T. Nguyen, D. Guillarme, S. Rudaz, J.L. Veuthey, J. Chromatogr. A 1128 (2006) 105.
[121] D. Guillarme, D.T.T. Nguyen, S. Rudaz, J.L. Veuthey, Eur. J. Pharm. Biopharm. 66 (2007) 475.
[122] M.J. Wirth, J. Chromatogr. A 1148 (2007) 128.
[123] L.A. Colon, J.M. Cintron, J.A. Anspach, A.M. Fermier, K.A. Swinney, Analyst 129 (2004) 503.
[124] K.D. Patel, A.D. Jerkovich, J.C. Link, J.W. Jorgenson, Anal. Chem. 76 (2004) 5777.
[125] A.D. Jerkovich, J.S. Mellors, J.W. Thompson, J.W. Jorgenson, Anal. Chem. 77 (2005) 6292.
[126] F. Gritti, G. Guiochon, Anal. Chem. 81 (2009) 2723.
[127] K. Kaczmarski, F. Gritti, J. Kostka, G. Guiochon, J. Chromatogr. A 1216 (2009) 6575.
[128] F. Gritti, G. Guiochon, J. Chromatogr. A 1216 (2009) 1353.
[129] J.H. Dymond, R. Malhotra, Int. J. Thermophys. 9 (1988) 941.
[130] M. Martin, G. Guiochon, J. Chromatogr. A 1090 (2005) 16.
[131] A.J. Easteal, AIChE J. 30 (1984) 641.
[132] B.A. Bidlingmeyer, R.P. Hooker, C.H. Lochmuller, L.B. Rogers, Sep. Sci. 4 (1969) 439.
[133] T.A. Maldacker, L.B. Rogers, Sep. Sci. 9 (1973) 27.
[134] G. Prukop, L.B. Rogers, Sep. Sci. 13 (1978) 59.
[135] F. Gritti, C.A. Sanchez, T. Farkas, G. Guiochon, J. Chromatogr. A 1217 (2010) 3000.
[136] K.J. Fountain, U.D. Neue, E.S. Grumbach, D.M. Diehl, J. Chromatogr. A 1216 (2009) 5979.
[137] F. Gritti, G. Guiochon, J. Chromatogr. A 1217 (2010) 7677.
[138] S. Fekete, J. Fekete, J. Chromatogr. A 1218 (2011) 5286.
[139] Y. Zhang, X. Wang, P. Mukherjee, P. Petersson, J. Chromatogr. A 1216 (2009) 4597.
[140] D.V. McCalley, J. Chromatogr. A 1218 (2011) 2887.
[141] J.O. Omamogho, J.D. Glennon, Anal. Chem. 83 (2011) 1547.
[142] A. de Villiers, F. Lynen, P. Sandra, J. Chromatogr. A 1216 (2009) 3431.